Int. J. Solids Structures Vol. 25, No. 7, pp. 769–782, 1989
Printed in Great Britain.

0020-7683/89 $3.00 + .00

DYNAMIC PLASTIC DEFORMATION IN STRAIN-HARDENING AND STRAIN-SOFTENING CANTILEVERS

W. J. STRONGE and T. X. YU†
University of Cambridge, Department of Engineering, Trumpington Street, Cambridge CB2 1PZ, U.K.

(*Received* 23 *June* 1988; *in revised form* 12 *November* 1988)

Abstract—The collision of a missile on a deformable cantilever results in a transient followed by a modal stage of plastic deformation. A theory for strain-hardening (softening) structures that separates the cantilever into a deforming and a rigid segment results in a distribution of deformation for the transient stage that is quite different from the results of a perfectly plastic structural model. Nevertheless, strain-hardening (softening) only slightly increases (decreases) the part of the initial kinetic energy dissipated during the transient stage. The modal stage of deformation for a strain-hardening body exhibits diffuse "plastic hinges" whereas a strain-softening body always has deformation that finally focuses at a point. Except for the extent of the deforming region, the modal configurations for strain-hardening and strain-softening structures are almost the same.

INTRODUCTION

The collision of a rigid missile on a slender structural element results in at least two stages of deformation: an initial transient stage where a disturbance travels away from the impact point and a later "modal" stage where the spatial distribution is independent of time. These stages of dynamic plastic deformation were clearly defined in Parkes' (1955) analysis of transverse impact at the tip of a rigid perfectly plastic cantilever. Part of the elegance of Parkes' solution was a result of the constitutive idealization he considered; a rigid perfectly plastic moment curvature relation substantially simplified the kinematic analysis by localizing all deformation in a "plastic hinge" that travelled away from the impact point. The hinge slowed as it moved away from the tip and became stationary when it reached the root of the cantilever. When a particle with mass G struck the cantilever with mass ρL, Parkes showed that the final distribution of deformation depended on the mass ratio. With light missiles ($G/\rho L \ll 1$) most of the initial kinetic energy was dissipated between the ends of the beam during the first stage of deformation, whereas with heavy missiles ($G/\rho L > 1$) almost all of the energy was dissipated in a modal configuration during the second stage. Experiments on mild steel beams exhibited these same response characteristics.

Additional impact experiments were performed on mild steel and aluminium alloy cantilevers by Mentel (1958), Cowper and Symonds (1957), Hall *et al.* (1971) and Bodner and Symonds (1962). They concluded that discrepancies between the measured deflections and predictions of the rigid–plastic theory could be explained as the effects of strain-rate and large deflection. Strain-hardening was deemed to be a less significant influence on the deformations of these slender cantilevers.

Static analyses of flexural plastic deformations in thin structural elements have shown that strain-hardening diffuses the stationary plastic hinges. The plastically deforming regions spread through a finite volume of material as deformation increases (Reid and Reddy, 1978a, b; Yu, 1979). If the moment at every section monotonically increases, these analyses of one-dimensional strain-hardening structural elements are indistinguishable from nonlinear elastic analyses. A decrease of the moment within plastically deforming regions can be caused by dynamic effects or geometric changes due to large deflections. When this occurs the section unloads along a different moment–curvature path from monotonic loading; the unloading path preserves the current value of the plastic curvature. Wu and Yu (1986) have shown that this irreversible aspect of plasticity localizes plastic deformation in statically loaded cantilevers when the tip deflection becomes large. Localization mostly affects the cantilevers that are not very flexible.

† On leave from Department of Mechanics, Peking University, Beijing, China.

The dynamic deformation of strain-hardening beams was considered by Conroy (1952) who commented that "an infinite number of localized plastic regions form along the beam". Later analyses of impulsively loaded beams by Florence and Firth (1965) and Forrestal and Sagartz (1978) obtained solutions by circumventing the difficulty that was present in transient solutions; they only considered strain-hardening during the modal stage of deformation. These authors estimated the dynamic response by assuming strain-hardening did not influence the spatial distribution of deformation. Jones (1967) extended this kinematic approximation to include the transient stage of deformation by spreading "moving hinges" over a predetermined length of beam. These approximations for the plastic deformation in strain-hardening beams do not satisfy the yield condition at all times; nevertheless, the approximations probably provide reasonable estimates for final deflections if the strain-hardening modulus is small.

Strain-hardening moment–curvature relations for plastically deforming structures are constitutive idealizations that represent a material property and cross-sectional characteristics. Strain-softening, on the other hand, is an effect caused by either microstructural or structural damage in a cross-section; this damage depends on strain (Krajcinovic, 1979). Sandler (1984) made the point that strain-softening is not a material property. Softening caused by the growth or multiplication of flaws has a natural or characteristic length associated with the flaw size or spacing. Although these details are swept aside by continuum hypotheses, analyses of strain-softening continua naturally present a requirement for a characteristic minimum size of the deforming region. Without this constraint, analyses of strain-softening continua result in localization of plastic deformation in a vanishingly small region (Bazant, 1976; Bazant and Belytschko, 1985). This localization is a manifestation of a material instability. Hence, continuum analyses require an artificial lower limit on the size of the plastically deforming region to ensure a positive rate of energy dissipation. This size effect also causes convergence problems for finite element discretizations of structures that exhibit strain-softening; the element size can never be small enough so there is a representative material property for those elements containing the localized plastically deforming region (Schreyer and Chen, 1986; Pietruszczak and Mroz, 1981). These numerical analyses achieve convergence for local, rate-independent constitutive relations by once again introducing some characteristic size or thickness for the strain-softening region. Wood (1968) has described how this same artifice (limitation of localization) was previously used to achieve stability in static analyses of damageable concrete beams and plates.

The present investigation primarily explains the influence of strain-hardening and strain-softening on the transient stage of dynamic plastic deformation. For a collision at the tip of a rigid strain-hardening (softening) cantilever, the entire body is instantaneously loaded to the initial yield moment M_0 when the collision occurs. Deformations begin throughout the cantilever at this instant. The deformations are accompanied by transverse accelerations that are large at sections near the tip and insignificant near the root. These accelerations soon reduce the bending moment near the tip to less than the current yield moment so a rigid segment quickly emerges from the tip. This previously deformed but currently rigid segment grows from the tip until it envelops most of the cantilever. The curvature at any section develops *before* it becomes a part of the rigid segment; all sections in the rigid segment are unloading from a previously deformed state. Hence, the bending moment first increases and then decreases at all sections that are not very near the root. The curvature developed at each section during this cycle is uniquely defined for strain-hardening beams; the picture is not so clear for strain-softening structural elements. At a deforming section in a strain-softening cantilever, the change in the bending moment with time must be negative for both loading and unloading paths (Fig. 1). The loading and unloading paths are associated with increasing curvature and no further change in curvature, respectively. Hence, the sign for the rate-of-change in bending moment cannot be used as a criterion to distinguish loading and unloading. The theory developed here solves this dilemma by separating the cantilever into two regions: (a) a rigid segment of increasing length that spreads from the tip, and (b) a deforming segment that shrinks toward the root. We assume that the root segment is loading and the tip segment is unloading, i.e. all deformation develops in the root segment. Furthermore, inertial effects are neglected in the

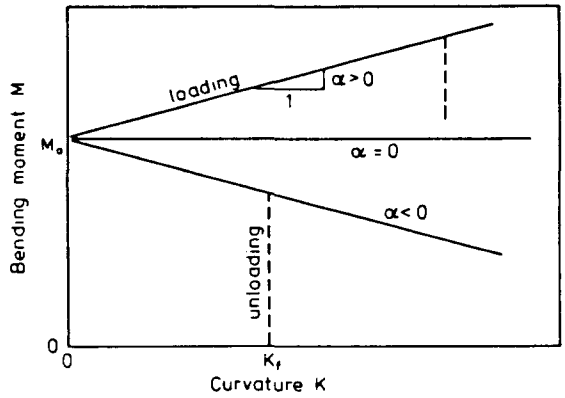

Fig. 1. Moment–curvature relations for strain-hardening and strain-softening rigid–plastic sections.

slowly moving root segment. This theory for plastic deformation of both strain-hardening and strain-softening structural elements results in dynamics for the transient stage that converge to Parkes' solution as the hardening parameter α vanishes.

PROBLEM SETTING AND THEORY

A uniform cantilever of length L and mass per unit length ρ carries a particle with mass G fixed to the tip (see Fig. 2). The cantilever has material properties that can be represented by one of the rigid–plastic moment–curvature relations shown in Fig. 1. This idealization has two properties: a yield moment M_0 and a strain-hardening modulus α

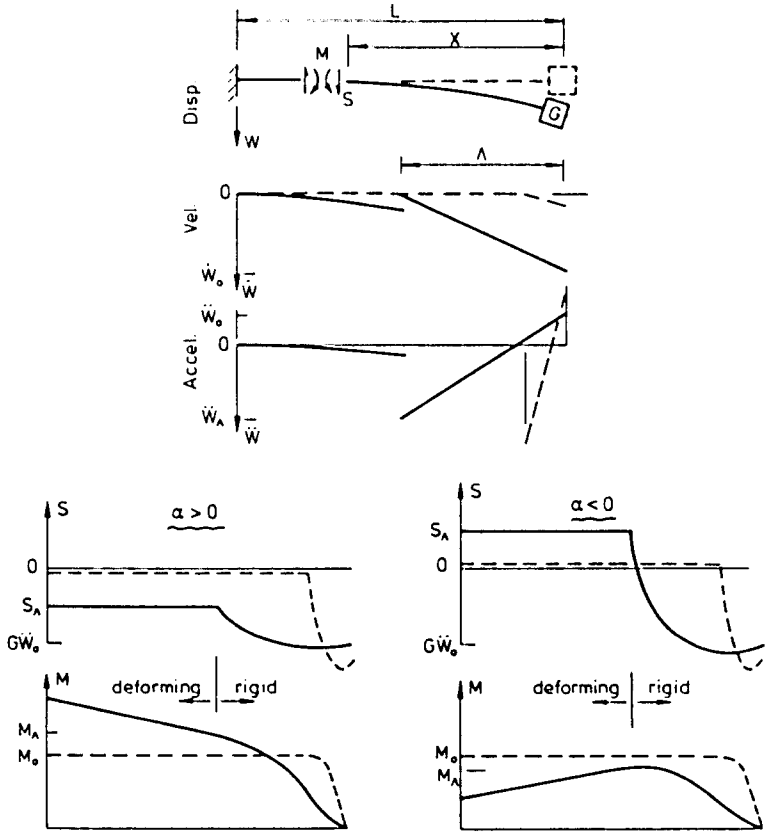

Fig. 2. Displacement, velocity, acceleration, shear resultant and bending moment distributions for impulsively loaded cantilevers during the transient stage. The dashed lines represent these variables at a very early time.

where α can be either positive or negative. Curvature $K = K(X, t)$ can develop at any section of the cantilever only after the bending moment M has been equal to M_0. Thereafter, a section either deforms with a change in moment that follows a loading path or the section unloads without further deformation if the moment is less than the current yield moment $M_y = M_0 + \alpha K$. The solid lines on Fig. 1 represent loading paths where $\dot{K} = \mathrm{d}K/\mathrm{d}t > 0$, while the dashed lines are unloading paths where $\dot{K} = 0$. The moment–curvature relation for the loading and unloading paths can be expressed as

$$M = M_0 + \alpha K, \quad \dot{K} > 0$$
$$M < M_0 + \alpha K, \quad \dot{K} = 0. \tag{1}$$

The unloading path simply maintains the largest curvature previously developed.

Impact suddenly imparts a transverse velocity V_0 to the particle at the tip while the remainder of the cantilever is at rest. The propagation of this disturbance away from the tip depends on inertia. Guided by Parkes' analysis, we assume that at any time t the velocity disturbance is only significant within a length Λ from the tip and that the cantilever length is composed of two segments: an undeforming segment $0 < X < \Lambda$ and a plastically deforming segment $\Lambda < X < L$ (see Fig. 2). As the interface Λ moves from the tip towards the root, a section located at distance X from the tip begins to deform on the loading path at $t = 0$ and stops deforming when $\Lambda(t) = X$. Furthermore, we assume that the inertia of the deforming segment $\Lambda < X < L$ is negligible. Since the segment near the tip is rigid, the transverse velocity $\dot{W}(X, t) = \mathrm{d}W/\mathrm{d}t$ can be expressed as

$$\dot{W} = V(1 - X/\Lambda), \quad X \leqslant \Lambda \tag{2}$$

where the tip velocity $V(t) = \dot{W}(0, t)$. The neglect of inertia effects in the deforming segment is reasonable since the velocities there remain small in comparison with velocities near the tip (Ting, 1964).

The shear force $S(X, t)$ is uniform in the deforming segment $\Lambda < X < L$ when inertia is negligible as shown in Fig. 2. At the interface between deforming and rigid segments this force $S_\Lambda = S(\Lambda, t)$ either increases or decreases monotonously with time depending on the sign of α. Consequently, the bending moment $M(X, t)$ also either increases or decreases linearly with X depending on the hardening parameter. The moment at the interface M_Λ is determined by the curvature $K(\Lambda, t) = \partial^2 W/\partial X^2$ that is developed before $\Lambda(t) = X$:

$$M_\Lambda = M_0 + \alpha K_\Lambda. \tag{3}$$

PLASTIC DEFORMATION OF ROOT SEGMENT

Since inertial forces are neglected in the deforming region, the bending moment varies linearly with distance from the deforming–undeforming interface at any instant of time.

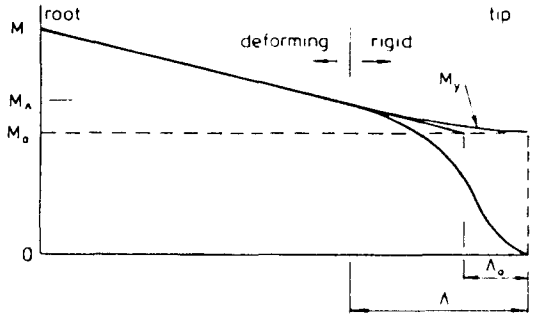

Fig. 3. Bending moment distribution for strain-hardening cantilever during the transient stage. The related final curvature K is related to the residual yield moment M_y by $K = (M_y - M_0)/\alpha$.

$$M = M_0 - S_\Lambda(X-\Lambda_0), \quad \Lambda \leqslant X \leqslant L \tag{4}$$

where $\Lambda_0(t)$ is the intersection of $M(x)$ with M_0 that is shown in Fig. 3. This figure shows typical distributions for M and the residual yield moment M_0, at an instant during the transient stage. At each instant the curvature in the deforming region is related to the shear resultant at the interface by

$$\alpha \frac{\partial^2 W}{\partial X^2} = -S_\Lambda(X-\Lambda_0). \tag{5}$$

At any time the inclination of the beam $W'(X,t) = \partial W/\partial X$ can be obtained by integrating eqn (5) and applying the boundary condition $W'(L,t) = 0$,

$$W' = -S_\Lambda(2\Lambda_0 - L - X)(L-X)/2\alpha. \tag{6}$$

Thus the angular velocity in the deforming region is

$$\dot{W}' = -[\dot{S}_\Lambda(2\Lambda_0 - L - X) + 2S_\Lambda\dot{\Lambda}_0](L-X)/2\alpha \tag{7}$$

and at the interface

$$\dot{W}'_\Lambda = -[\dot{S}_\Lambda(2\Lambda_0 - L - \Lambda) + 2S_\Lambda\dot{\Lambda}_0](L-\Lambda)/2\alpha. \tag{8}$$

An additional relationship is required at the interface to ensure that the distribution of final curvature at sections that are finally in the rigid segment is an analytic function. Therefore from (5),

$$0 = \mathrm{d}M_\Lambda/\mathrm{d}\Lambda_0 = S_\Lambda - (\Lambda - \Lambda_0)\,\mathrm{d}S_\Lambda/\mathrm{d}\Lambda_0. \tag{9}$$

This constitutive constraint results in an expression for the angular velocity at the interface,

$$\dot{W}'_\Lambda = +\dot{S}_\Lambda(L-\Lambda)^2/2\alpha. \tag{10}$$

DYNAMICS OF EXPANDING SEGMENT NEAR THE TIP

The expanding segment $0 < X < \Lambda(t)$ is presumed to be unloading so that no further deformation occurs. *A posteriori* we will confirm that at every section throughout this region, the moment is always less than the magnitude of M_Λ when the section entered the segment. This rigid segment rotates with an angular velocity $\mathrm{d}\dot{W}_\Lambda/\mathrm{d}X$. Hence the velocity of the tip is

$$V = -\dot{S}_\Lambda\Lambda(L-\Lambda)^2/2\alpha. \tag{11}$$

Neglecting the small transverse velocity at the moving interface, we assume the velocities and accelerations in the rigid segment are given by

$$\dot{W}(X,t) = V(1-X/\Lambda) \tag{12}$$

$$\ddot{W}(X,t) = \dot{V}(1-X/\Lambda) + VX\dot{\Lambda}/\Lambda^2, \quad 0 \leqslant X \leqslant \Lambda. \tag{13}$$

These accelerations cause a shear resultant at the interface,

$$S_\Lambda = (G + \rho\Lambda/2)\dot{V} + \rho\dot{\Lambda}V/2. \tag{14}$$

Likewise, the moment at the interface is

$$M_\Lambda = -\Lambda S_\Lambda - \rho\Lambda(\Lambda\dot{V} + 2\dot{\Lambda}V)\ 6. \tag{15}$$

This moment is the same as the moment M_Λ at the end of the deforming segment, eqn (4), so

$$M_0 + \Lambda_0 S_\Lambda = \rho\Lambda(\Lambda\dot{V} + 2\dot{\Lambda}V)\ 6. \tag{16}$$

These relations for the rotating rigid segment near the tip are the same as those for Parkes' problem if $S_\Lambda = 0$.

NON-DIMENSIONAL EQUATIONS FOR DYNAMIC SYSTEM

The differential equations (9), (11), (14) and (15) for the unknown functions $V(t)$, $S_\Lambda(t)$, $\Lambda(t)$ and $\Lambda_0(t)$ can be expressed in terms of non-dimensional variables

$$v = V/V_0, \quad s = S_\Lambda L/M_0, \quad \lambda = \Lambda/L, \quad \lambda_0 = \Lambda_0/L \tag{17}$$

and characteristic parameters for the system

$$\zeta = G/\rho L, \quad \gamma = \alpha LM_0, \quad \beta = GV_0^2/2M_0, \quad t_0 = \rho L^2 V_0/M_0. \tag{18}$$

It will be useful to supplement these natural ratios with an additional parameter that combines the strain hardening and impact energy ratios, $\phi = \beta\gamma$. Also, notation indicating differentiation with respect to time is defined as

$$\dot{\Lambda} = \mathrm{d}\Lambda/\mathrm{d}t \quad \text{and} \quad \dot{\lambda} = \mathrm{d}\lambda/\mathrm{d}\tau \quad \text{where } \tau = t/t_0.$$

The equations describing the dynamics of the system with these nondimensional variables are

$$\dot{s}(\lambda - \lambda_0) = s\dot{\lambda}_0 \tag{19}$$

$$\dot{s}\lambda(1-\lambda)^2 = -4\phi v/\zeta \tag{20}$$

$$\frac{\mathrm{d}}{\mathrm{d}\tau}(2\zeta v + \lambda v) = 2s \tag{21}$$

$$\frac{\mathrm{d}}{\mathrm{d}\tau}(\lambda^2 v) = 6(1 + \lambda_0 s). \tag{22}$$

These first-order equations can be rearranged in a form that is convenient for integration.

$$\dot{\lambda}_0 = -4\phi v(\lambda - \lambda_0)/\zeta s\lambda(1-\lambda)^2 \tag{23}$$

$$\dot{\lambda} = 2\{3(2\zeta + \lambda) + [3\lambda_0(2\zeta + \lambda) - \lambda^2]s\}/\lambda v(4\zeta + \lambda) \tag{24}$$

$$\dot{s} = -4\phi v/\zeta\lambda(1-\lambda)^2 \tag{25}$$

$$\dot{v} = -2[3 + (3\lambda_0 - 2\lambda)s]/\lambda(4\zeta + \lambda). \tag{26}$$

The initial conditions for this problem with a shear resultant that is compatible with the moment distribution shown in Fig. 2 are

$$\lambda_0 = \lambda = s = 0 \quad \text{and} \quad v = 1 \quad \text{for } \tau = 0. \tag{27}$$

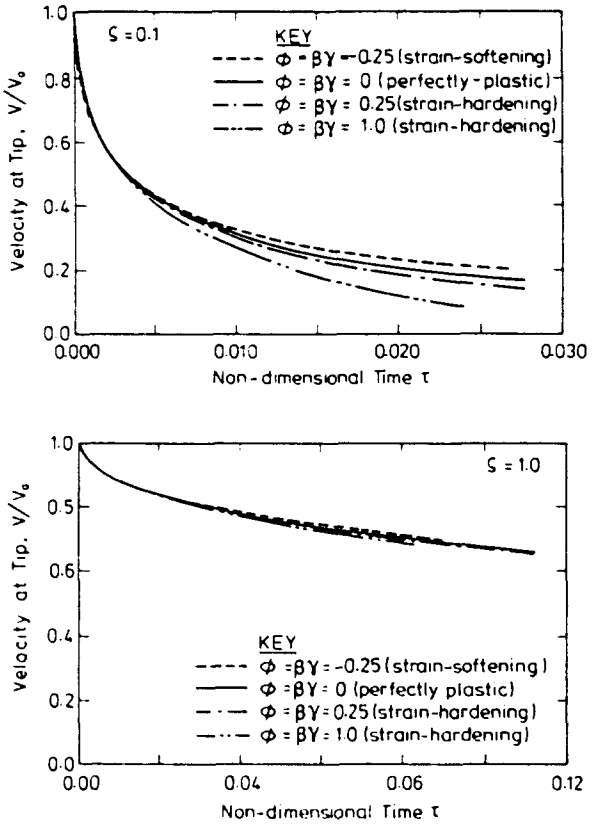

Fig. 4. Velocity of tip during the transient stage for light and intermediate mass ratios, $\zeta = G/\rho L$.

Differential equations for the system are singular for these initial conditions. Soon after the initial impact, however, eqn (23) can be approximated by

$$\dot{\lambda} = 3/\lambda \quad \text{for } \tau \ll 1;$$

that is, the interface moves away from the tip with a speed that decreases with distance. It follows that

$$\lambda = \sqrt{(6\tau)} \tag{28}$$

and from eqn (26)

$$\dot{v} = -3/2\zeta\lambda = -3/2\zeta\sqrt{(6\tau)}.$$

Hence the tip speed initially decreases from the impact speed as

$$v = 1 - \sqrt{(6\tau)}/2\zeta. \tag{29}$$

The shear resultant at the interface and the hardening parameter λ_0 can be obtained in the same manner.

$$s = -4\phi\sqrt{(6\tau)}/3\zeta \tag{30}$$

$$\lambda_0 = \sqrt{(6\tau)}/2 \quad \text{for } \tau \ll 1. \tag{31}$$

Figure 4 shows the tip velocity during the entire transient stage for impulsively loaded

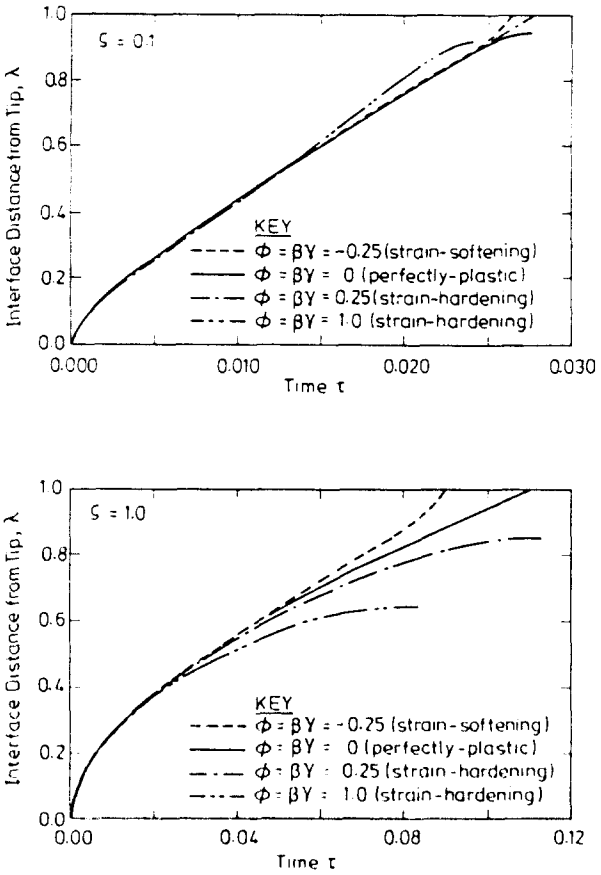

Fig. 5. Travel of loading–unloading interface away from tip during the transient stage for light and intermediate mass ratios.

cantilevers. Both the duration and the decrease in tip speed for this stage are primarily influenced by the mass ratio ζ. When $\zeta \ll 1$, most of the initial velocity disappears while λ is increasing; in contrast, when the mass ratio is moderate to large $\zeta \geqslant 1$, neither the rate-of-impulse imparted by the shear force nor the inertia of the beam that enters the rigid segment are large in comparison with the inertia of the mass at the tip, so strain-hardening mostly affects the length of the rigid segment (Fig. 5). It only slightly increases the deceleration of the tip.

END OF INITIAL TRANSIENT STAGE

The interface between rigid and deforming segments of the cantilever travels away from the tip during an initial transient stage of deformation. For strain-hardening cantilevers $\alpha > 0$, this stage terminates when $\dot{\lambda} = 0$. The interface terminus $\lambda_1 < 1$ can be determined from eqn (24).

$$\lambda_1^2(2\zeta + \lambda_1)^{-1} = 3(\lambda_{01} + s_1^{-1}) \tag{32}$$

where $\lambda_{01} = \lambda_0(\tau_1)$ and $s_1 = s(\tau_1)$. The terminal position depends on the hardening parameter ϕ and the mass ratio ζ as shown in Fig. 6. The subsequent stage of motion has deformation only in the region $\lambda_1 < x < 1$. This region spreads from the root as the hardening parameter α and the initial kinetic energy β increase.

For a strain-softening body $\alpha < 0$, the condition for a stationary finite-length plastically deforming region (eqn (32)) is never satisfied. Hence, the first stage terminates when $\lambda = 1$ and the second stage of motion has deformation condensed into a point at the root of the beam.

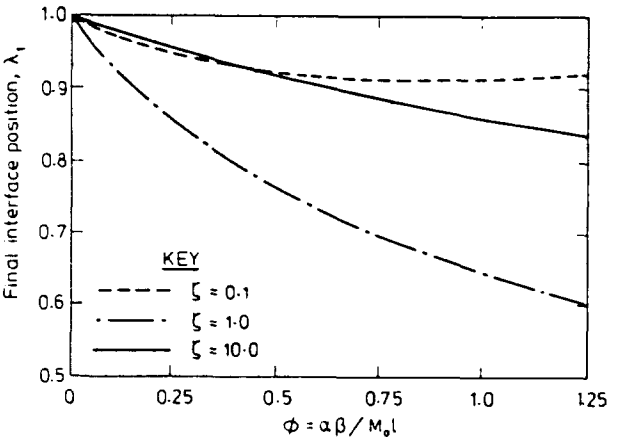

Fig. 6. Length of the rigid segment during the modal stage of deformation.

At the end of stage I the residual kinetic energy $E_1 = E(\tau_1)$ can be compared with the initial kinetic energy $E_0 = GV_0^2/2$.

$$\frac{E_1}{E_0} = \left(1 + \frac{\lambda_1}{3\zeta}\right) v_1^2. \tag{33}$$

Figure 7 shows that the energy dissipated during the transient stage is remarkably insensitive to the hardening parameter unless the colliding mass G is very light. For a small mass ratio ζ where most of the kinetic energy is dissipated by bending away from the root, strain-hardening increases the part of the total energy dissipated during the initial stage of deformation. Strain-softening, on the other hand, reduces the part of the initial kinetic energy that is dissipated by distributed bending during stage I.

"MODAL" STAGE OF DEFORMATION

The remaining kinetic energy E_1 is dissipated in a stationary mode of deformation during the period $\tau_1 < \tau < \tau_2$ where the final time τ_2 is determined by $v(\tau_2) = 0$. For this period, deformation continues to develop in the segment $\lambda_1 < x < 1$ of a strain-hardening cantilever. Since we assume that inertia is negligible in this region, the shear resultant is uniform and the bending moment increases linearly with distance from the interface terminus λ_1. The initial moment $m_* = 1 - (\lambda_1 - \lambda_{01})s_1$ at the terminus can be used to express the moment $m_1(x, \tau_1)$ within the root segment at the beginning of stage II.

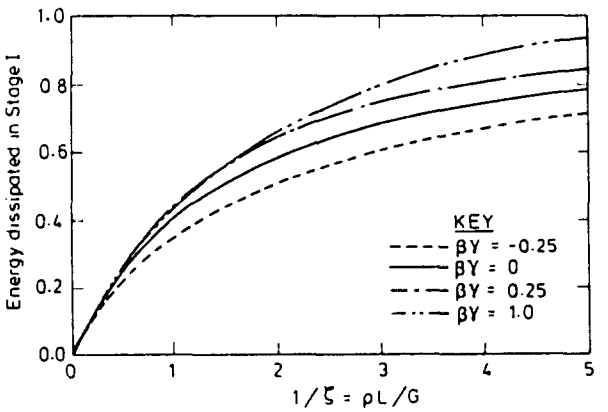

Fig. 7. The part of the initial kinetic energy that is dissipated during the transient stage.

$$m_1 = m_* - (x-\lambda_1)s_1(\lambda_1, \tau_1), \quad \lambda_1 \leqslant x \leqslant 1. \tag{34}$$

The moment at any section increases monotonously from an initial value $m_1 = m_1(x, \tau_1)$ to the final state $m_2 = m_2(x, \tau_2)$. To satisfy the equations of motion in the rigid segment, the moment $m(\lambda, \tau)$ and the shear resultant $s(\lambda_1, \tau)$ at the stationary interface must vary proportionately during stage II. The bending moment $m_2(x, \tau_2)$ in the deforming segment when motion finally stops is

$$m_2 = m_1 s_2 / s_1. \tag{35}$$

A change in curvature at every section $K_2 - K_1 = M_0(m_2 - m_1)/\alpha$ corresponds to the increase in the bending moment during stage II. The energy dissipated by this plastic deformation equals the kinetic energy E_1 of the system at the beginning of this stage.

$$\begin{aligned} E_1 &= \frac{M_0^2 L}{2\alpha}\int_{\lambda_1}^{1}(m_2^2 - m_1^2)\,\mathrm{d}x \\ &= \frac{M_0^2 L}{6\alpha}\left[1 - \frac{m_*}{s_1(1-\lambda_1)} + \frac{m_*^2}{s_1^2(1-\lambda_1)^2}\right](s_2^2 - s_1^2)(1-\lambda_1)^3. \end{aligned} \tag{36}$$

It follows that the final shear resultant s_2 can be obtained from s_1 and eqns (33)–(35).

$$s_2 = -\left\{s_1^2 + 2\phi(1+\lambda_1/3\zeta)v_1^2(1-\lambda_1)^3\left[1 - \frac{m_*}{s_1(1-\lambda_1)} + \frac{m_*^2}{s_1^2(1-\lambda_1)^2}\right]^{-1}\right\}^{\frac{1}{2}}.$$

The change in moment during stage II is obtained from this shear resultant. Thus, the final curvature is completely determined by conditions at the beginning of the final stage because the deformation is a separable function of spatial and temporal variables during this stage.

The hypotheses in this theory that prescribe the initial and boundary conditions for stage II are consistent with the hypotheses that separate the cantilever into deforming and rigid segments. A consequence of this approximation is a discontinuity in bending moment at λ_1. This discontinuity develops during stage II with strain-hardening.†

A fundamental problem arises when finding the motion of a strain-softening cantilever during stage II, after the deforming region shrinks to a point. The deforming region has no length so any further deformation results in an indefinitely large curvature and no energy dissipation. Other investigations have circumvented this problem by specifying a minimum length for the deforming region and defining a moment–curvature relation which asymptotically approaches a positive moment as the curvature increases. Alternatively, a different constitutive relation can be defined for the localized region, i.e. a moment–rotation rather than a moment–curvature relation (Martin, 1988). Parkes' analysis of the second stage followed the latter route. Neither of these paths develops from the constitutive relations considered here so we have not calculated any final deflections for strain-softening cantilevers.

CALCULATION OF DYNAMIC RESPONSE

The time-dependent behaviour of the system during stage I was examined by solving eqns (23)–(26) using a Runge–Kutta procedure. Initial conditions (28)–(31) were used to start this calculation at time $\tau = 10^{-12}$. Thus, the motion of the cantilever and its moment distribution were calculated as functions of time for typical values of the impact parameters.

The final curvature at sections $0 \leqslant x \leqslant \lambda_1$ was obtained from the moment M_1 when the section passed into the rigid (unloading) region. The root section of strain-hardening

† The condition $\dot{\lambda} < 0$ for $\tau > \tau_1$ is not possible since it results in a negative rate of energy dissipation.

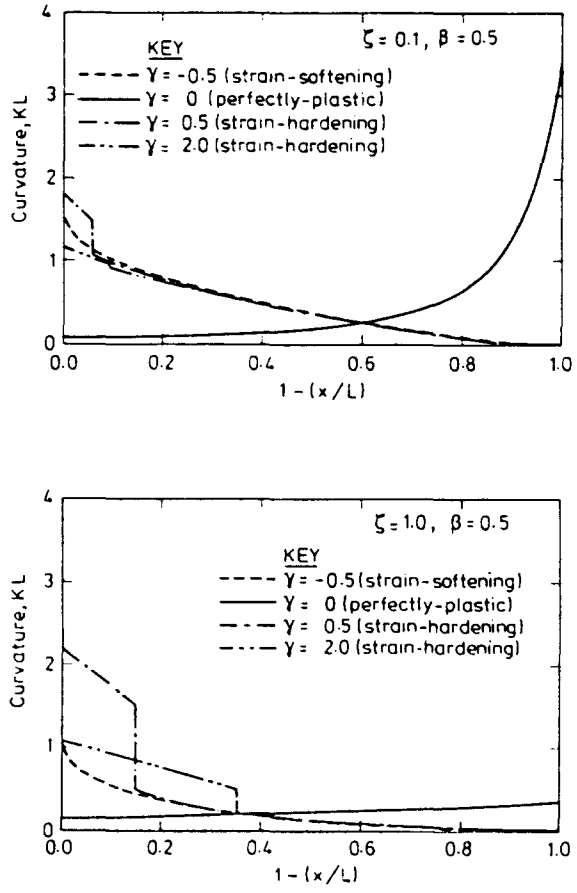

Fig. 8. Final distribution of curvature for an energy ratio $\beta = GV_0^2/2M_0 = 0.5$.

cantilevers continues to deform while $t > 0$ so the curvatures in the section $\lambda_1 < x \leqslant 1$ increase until the final time τ_2.

RESULTS AND DISCUSSION

The deformation of strain-hardening cantilevers is shown in Fig. 8 for mass ratios $\zeta = 0.1$ and 1.0. With a heavy mass, most of the initial kinetic energy is dissipated during stage II; the small part dissipated in the transient stage is almost independent of the hardening coefficient α. However, the hardening coefficient does influence the extent of the deforming segment at the root during the second stage; the length of this segment increases with α and the increased length of the deforming material tends to diminish the increase in curvature during this stage. Consequently the effect of strain-hardening on final tip deflection is more when the mass ratio is large as shown in Fig. 9. With a light mass $\zeta < 0.5$, most of the impact energy is dissipated in distributed curvature that develops during the transient stage of motion. Figure 7 shows that strain-hardening accentuates this effect, that is the fraction of the impact energy dissipated in stage II decreases as hardening increases. Strain-softening has an unusual effect only at the last of the transient stage when the interface is almost at the root. Then the shear resultant s_1 increases very rapidly and there is a concomitant final increase in curvature near the root.

The discontinuities in curvature that arise at λ_1 during the modal stage are not apparent in the final deformed configurations (Fig. 9). These deformed profiles show that strain-hardening decreases the deformation; the only apparent effect on the distribution of curvature is the extent of the stage II deforming region when there is a large mass at the tip. The strain-hardening coefficient α and the initial kinetic energy ratio β have exactly the same effect on the distribution of deformation for all stages of the dynamic response. Hence,

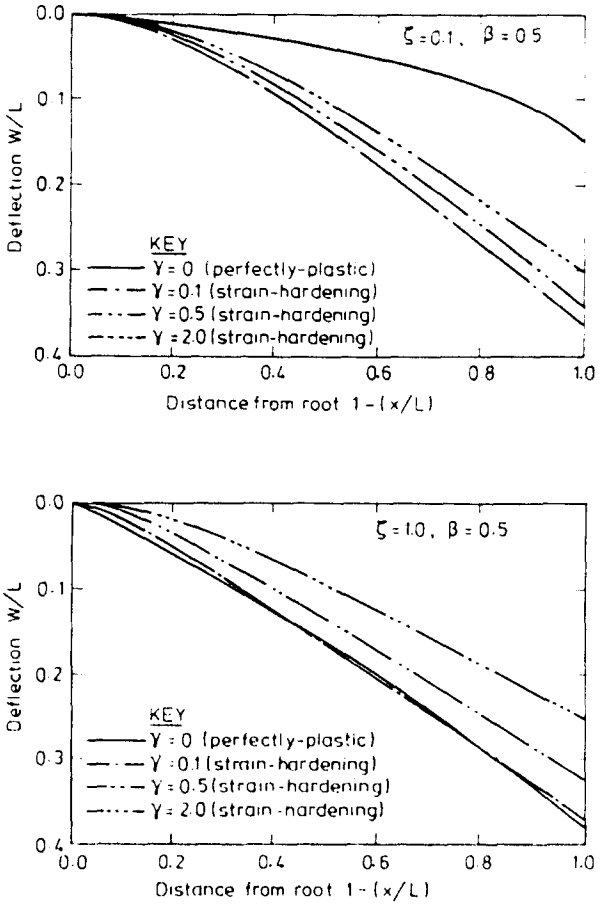

Fig. 9. Final deflection of impulsively loaded, strain-hardening cantilevers for light and intermediate mass ratios.

the final deformation is directly proportional to β and the effect of increasing β on the distribution of curvature is equivalent to a proportional increase in α.

Calculations for the distribution of final curvature in strain-hardening and strain-softening cantilevers have been compared with Parkes' theory in Fig. 8. The present theory yields curvature which increases towards the root while the curvature in the perfectly plastic theory increases with distance from the root. These distinctly different behaviours result from similar hypotheses; the difference is a consequence of the assumed moment–curvature relation. Parkes' theory assumes that all deformation occurs at a hinge which travels away from the tip. The segment ahead of the hinge does not deform although the entire segment is at yield. Our extension of the theory that considers strain-hardening and strain-softening *requires* deformations throughout the entire root segment; the curvature of the cantilever increases towards the root as a consequence of the *static* bending moment in the stationary segment.

In the limit as the hardening (softening) parameter α vanishes, the dynamic deformation of a strain-hardening cantilever continues to have a distribution of curvature which is larger near the root whereas the perfectly plastic cantilever has larger curvature near the tip. Despite this difference, these cantilevers have exactly the same energy dissipated by distributed deformation during stage I in the limit as $\alpha \to 0$.

Experiments and numerical analyses of impact on elasto-plastic cantilevers tend to exhibit more curvature near the tip in agreement with the perfectly plastic results. Reid and Gui (1987) calculated results for an elastic-perfectly plastic cantilever with a light mass at the tip. This showed an initial stage of dynamic deformation where plastic strains developed only in a short segment that travelled away from the tip. Although this may be interpreted as a diffuse "plastic hinge", the bending moment ahead of the deforming segment was not

similar to that of the rigid–perfectly plastic theory. The results showed that the plastically deforming segment was confined by an elastic region. This pattern of confinement moved steadily away from the impact point at a speed that was somewhat less than the speed of a "plastic hinge". The deforming segment travelled away from the tip until there was interference with an elastic wave that was travelling in the opposite direction after reflection at the root. This pattern suggests a dynamic rigid–plastic model with a short plastically deforming region that travels away from the tip into undeformed sections of the cantilever. However, all such models were abandoned because they resulted in an underdetermined set of equations; there were insufficient boundary conditions to both locate and satisfy dependent variables at the ends of the deforming region.

We conclude that the rigid–perfectly plastic constitutive model is unique in predicting a distribution of curvature for the transient stage of deformation that exhibits elasto-plastic effects without incorporating elastic deformations. Our model is not realistic for the transient stage of deformation of either strain-hardening or strain-softening cantilevers because it neglects elastic effects. Nevertheless, the evolution of deformation towards a modal configuration clearly emerges. The present analysis does establish the distribution of curvature for the modal stage of deformation in strain-hardening cantilevers. This stage has a finite size for the deforming segment whereas a *strain-softening cantilever always exhibits localization of deformation into a point at the root*. For strain-softening structures where the bending stiffness remains positive, localized modal deformation can occur only at a finite distance from the impact point after a transient stage of deformation. Analyses of the modal stage for strain-softening structures require a constitutive relation with positive dissipation for increasing deformation; the bilinear moment–curvature relation considered here does not satisfy this condition after deformation focuses at a point. Hence only the transient stage of deformation for strain-softening structures has been analysed. For strain-hardening sections, the present analysis is reasonable when most of the deformation occurs in a modal configuration, that is when the colliding mass is not small.

REFERENCES

Bazant, Z. P. (1976). Instability, ductility and size effect in strain-softening concrete. *J. Engng Mech. ASCE* **EM2**, 331–334.

Bazant, Z. P. and Belytschko, T. B. (1985). Wave propagation in a strain-softening bar: exact solution. *J. Engng Mech. ASCE* **111**, 381–389.

Bodner, S. R. and Symonds, P. S. (1962). Experimental and theoretical investigation of the plastic deformation of cantilever beams subjected to impulsive loading. *J. Appl. Mech.* **29**, 719–728.

Conroy, M. F. (1952). Plastic rigid analysis of long beams under transverse impact loading. *J. Appl. Mech.* **19**, 465–470.

Cowper, G. R. and Symonds, P. S. (1957). Strain-hardening and strain-rate effects in the impact loading of cantilever beams. Division of Applied Mathematics, Brown University, TR28.

Forrestal, M. J. and Sagartz, M. J. (1978). Elastic–plastic response of 304 stainless steel beams to impulse loads. *J. appl. Mech.* **45**, 685–687.

Florence, A. L. and Firth, R. D. (1965). Rigid–plastic beams under uniformly distributed impulses. *J. Appl. Mech.* **32**, 481–488.

Hall, R. G., Al-Hassani, S. T. S. and Johnson, W. (1971). The impulsive loading of cantilevers. *Int. J. Mech. Sci.* **13**, 415–430.

Jones, N. (1967). Influence of strain-hardening and strain-rate sensitivity on the permanent deformation of impulsively loaded rigid–plastic beams. *Int. J. Mech. Sci.* **9**, 777–796.

Krajcinovic, D. (1979). Distributed damage theory of beams in pure bending. *J. Appl. Mech.* **46**, 592–596.

Martin, J. B. (1988). Dynamic bending collapse of strain-softening cantilever beams. In *Structural Failure* (Edited by T. Wierzbicki and N. Jones), pp. 365–388. John Wiley Interscience.

Mentel, T. J. (1958). The plastic deformation due to impact of a cantilever beam with an attached tip mass. *J. Appl. Mech.* **25**, 515–524.

Parkes, E. W. (1955). The permanent deformation of a cantilever struck transversely at its tip. *Proc. R. Soc. Lond.* **A228**, 462–476.

Pietruszczak, S. and Mroz, A. (1981). Finite element analysis of deformation of strain-softening materials. *Int. J. Numer. Meth. Engng* **17**, 327–334.

Reid, S. R. and Gui, X. G. (1987). On the elastic–plastic deformation of cantilever beams subjected to tip impact. *Int. J. Impact Engng* **6**, 109–127.

Reid, S. R. and Reddy, T. Y. (1978a). Effect of strain-hardening on the lateral compression of tubes between rigid plates. *Int. J. Solids Structures* **14**, 213–225.

Reid, S. R. and Reddy, T. Y. (1978b). Effect of strain hardening on the large plastic deformation of a cantilever. *J. Appl. Mech.* **45**, 953–955.

Sandler, I. S. (1984). Strain softening for static and dynamic problems. In *Proc. ASME Symp. on Constitutive Equations: Micro, Macro and Comparative Aspects* (Edited by K. Willam), pp. 217–231, New Orleans. ASME, New York.

Schreyer, H. L. and Chen, Z. (1986). One-dimensional softening with localization. *J. Appl. Mech.* **53**, 791–797.

Ting, T. C. T. (1964). The plastic deformation of a cantilever with strain-rate sensitivity under impulsive loading. *J. Appl. Mech.* **31**, 38–42.

Wood, R. H. (1968). Some controversial and curious developments in the plastic theory of structures. In *Engineering Plasticity* (Edited by J. Heyman and F. Leckie), pp. 665–691. Cambridge University Press, Cambridge.

Wu, X. and Yu, T. X. (1986). The complete process of large elastic–plastic deflection of a cantilever. *Acta Mech. Sinica* **2**, 333–347.

Yu, T. X. (1979). Finite plastic deformation of a ring pulled diametrically. *Acta Mech. Sinica* (in Chinese) **11**, 88–91.